A Numerical Study of Transient Turbine Wake Interaction

Vincent Podeur[*], Dominic Groulx[*], Christian Jochum[**]

[*] Department of Mechanical Engineering, Dalhousie University
[**] Institut de Recherche Dupuy de Lôme (IRDL), ENSTA Bretagne

Abstract- The high turbulence level of the incoming flow on a turbine has a significant impact on its performances, leading to a decrease in the electrical power output. Therefore, perturbations carried in the wake of an upstream turbine may also have a significant impact on the downstream one. This problematic has already been addressed but with simplified approaches such as the Blade Element Momentum theory giving interesting results regarding power extraction but lacking some precision regarding definition of the structure of the wake and its effect on load variation on the turbine blades. To get a better understanding of the effect of unsteady asymmetric flow on a downstream turbine, fully transient simulations designed to study the effect of the wake of an upstream turbine on a downstream one were performed with a RANS *k*-ω SST turbulence model using ANSYS-CFX. Three different configurations were considered, namely the downstream turbine aligned with the upstream one, offset by 0.5*D*, and offset of 1*D*. A 10*D* clearance between both turbines was used. A horizontal axis tidal turbine (HATT) was used for the study. Results show that when fully in-line, the downstream turbine sees reduction in power coefficient by more than 69%, and temporal variation of this coefficient having a relative amplitude of more than 30%.

Keywords- Horizontal Axis Tidal Turbine (HATT), Transient CFD, Turbine Interaction, Wake

I. INTRODUCTION

As technologies for harnessing energy from the tides become mainstream, like wind turbine, solar panels and nuclear/thermal plants today, those tidal turbines will more than likely be installed in arrays to capture the maximum amount of tidal energy in those areas where the tidal energy is the densest [1]. Installing turbines closer together would offer other advantages such as reduction in required power cable lengths, potentially sharing modules between multiple turbines and smallest overall footprint (impact on wildlife and fisheries [2] restricted to a smaller area in consequence). Ultimately, all of this having a direct impact on the economics, and the operation and maintenance of tidal turbines and tidal energy [3].

Therefore, two or more turbines will necessarily be installed in close proximity on the seabed. This confinement will lead to unavoidable interaction between upstream turbines' wakes and downstream turbines [4]. The velocity deficit in in the wake, in conjunction with the increase in flow turbulence, will have an effect on the performance of the downstream turbine. Moreover, for a situation when the downstream turbine is only partially in the wake of the upstream one, it would be expected that the asymmetric flow seen by the turbine will induced asymmetric and varying load on the turbine blades.

It has been shown experimentally that the high turbulence level in the wake flow incoming on a downstream turbine has a significant impact on performance, leading to a decrease of up to 63% in the turbine performance (spacing between the in-line turbines from 2*D* and 6*D*) [5]. This figure highlights the fact that perturbation carried in the wake of the upstream turbine can have a significant impact on the downstream one.

This problematic has already been addressed numerically using simplified approaches such as the blade element momentum theory (BEMT) often coupled with a RANS CFD approach [6, 7]. These studies provide interesting results regarding power extraction, but as expressed in Leroux *et al.* [8], lack some precision regarding the physical modeling of the structure of the wake and its effect on overall turbine performance and localized load variation on turbine blades.

To get a better understanding of the effect of unsteady asymmetric wake flow on a downstream turbine, fully transient simulation with RANS turbulence physics were run using ANSYS-CFX. Because of the proven relevance of the results obtained in earlier works [8-10], turbulent closure *k*-*ω* SST model has been used. The model of turbine considered for this study is a horizontal axis tidal turbine (HATT), used by Doman *et al.* [11] and tested in the towing tank at the Kelvin hydrodynamics basin at Strathclyde University. In the numerical study, two of those turbines are position at a distance 10*D* form one another.

This paper will present the implementation of this model and the results of the numerical study. The question of upstream to downstream turbine interactions, including the predicted turbine performances for the configurations studied will be discussed.

II. NUMERICAL MODEL AND MODELING

A. Turbine Geometry

The turbine considered in this study is the one used by Doman *et al.* [11] and tested at Strathclyde University. The general dimensions of the turbine are given in Table 1 with a CAD rendering of it presented in Fig. 1. The blades are based on an NREL S814 profile, and for this study, blade roots were simplified to facilitate the meshing process. A much more detailed description of the blade geometry can be found in [9, 11] and will not be repeated here. Regarding the nacelle dimension, they were estimated from those papers.

B. Fluid Domain and Boundary Conditions

Two numerical domains were considered, both sharing the same depth and width of 2.5 m and 4.6 m respectively. The length varied between the domains. The first numerical domain contains only one turbine and has a total length of 12*D*. The turbine is positioned a distance 2*D* from the inlet, leaving 10*D* for the wake to developed and be observed.

The second numerical domain contains two turbines and has a total length of 17*D*. The upstream turbine is still positioned at a distance 2*D* from the inlet and is located at the origin *0* of the domain. The downstream turbine is position at a distance 10*D* behind the upstream turbine (in the flow direction - the *z* axis). It is positioned at the same height as the upstream turbine, but its position varies in the *x* direction depending on the configuration considered.

Table 1: Turbine Dimensions

Parameter	Dimension
Turbine diameter (*D*)	0.762 m
Hub diameter	0.15 m
Rotor depth	1.25 m
Nacelle length	1.70 m

Table 2: Boundaries Conditions

Boundary	Condition
Inlet	Steady normal flow: $U_0 = 1$ m/s Turbulence Intensity = 5%
Outlet	Relative pressure $P_{rel} = 0$ Pa
Tank walls	Free slip, velocity at wall = U_0
Turbine walls	No slip
Nacelle walls	No slip

Figure 1: Turbine CAD rendering.

Three configurations are considered: a first one where the turbine is perfectly aligned in-line with the upstream one, a second one where the downstream turbine is offset by 0.5*D* in the *x* direction, and a third one with an offset of 1*D*.

For both fluid domains, non-slip boundary conditions have been applied to the turbines and nacelles wall. For the sake of simplicity, free-slip conditions have been applied to the tank walls, those also mimic movement of the turbine assembly in a two tank better. These conditions are summed up in Table 2.

C. Turbulence Model

The turbulence model chosen for these Reynolds Average Navier-Stokes (RANS) equations-based simulations is the Shear Stress Transport (SST) *k-ω* model. This two-equation eddy-viscosity model has been shown to properly account for turbulence in the free stream down to the viscous sublayer level close to the turbine walls [10, 12, 13]. This versatility is interesting since both turbine performances, which depends on the modelling of the boundary layers on the walls, and wake behaviour in the free stream are of interest for this study.

D. Computational Mesh

The computational domain is divided in two sub-domains. A rotating sub-domain, which encloses the rotating part of the tidal turbines and a stationary sub-domain which encloses the rotating sub-domains and the nacelles (see Fig. 2). Both domains are meshed separately using the ANSYS meshing tool. An unstructured meshing method using tetrahedral element is used. To ensure the continuity between both domains, the general grid interface (GGI) method is applied on all their shared boundaries.

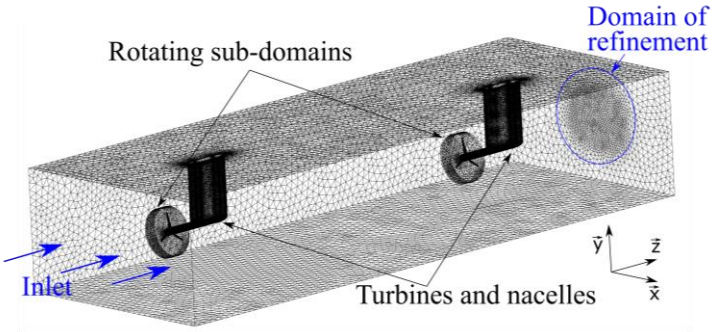

Figure 2: Meshed fluid domain.

Table 3: Mesh Information

Global meshing parameter	
Number of elements	23,785,687
Min element size	2.75×10^{-4} m
Max face size	0.15 m
Curvature Normal angle	7.5°
Max Wake cell size	4.5×10^{-2} m
Boundary layer meshing parameter	
Number of layers	30
Max thickness Blades	1.5×10^{-2} m
Max thickness Blades roots	1.5×10^{-2} m
Max thickness Hub	3×10^{-2} m
Max thickness Nacelle	5×10^{-2} m

To achieve an accurate modelling of the wake, a cylindrical domain of refinement is added in the wake of the turbine, starting right after the hub. This cylindrical domain has a diameter of 1.5*D* centered on the hub of the front turbine.

Since an extensive mesh convergence study and a validation of the results has been carried out on this exact turbine by Currie *et al.* [9], those meshing parameters were used as a reference for the present study. Details of the meshes used for both numerical domains are provided in Table 3. Of importance, the average y^+ values around the upstream and downstream turbines are 1.673 and 1.600 respectively. Since the Low-Reynold Number method has been used to model the near-wall region, these values are satisfactory. Indeed, for this method the first node of the mesh must be within the laminar sublayer, which is located at $y^+ < 11$.

E. Turbine Operation

For a single turbine in a uniform flow, simulations are performed at a given tip speed ratio (TSR); the turbine rotate at a rate that matches the TSR value for the given inlet flow velocity of 1 m/s in this work. Thus, a constant rotational speed is considered, and results are taken from the simulation once steady state, or quasi-steady state is reached; transient effects during the starting phase of the turbine while the flow velocity is increasing everywhere in the flow are not addressed.

For the two turbine simulations in a uniform inlet flow, the same approach is taken, the identical TSRs of both turbines are fixed, *i.e.*, both turbines rotate at a constant identical rotation rate. Looking specifically at the downstream turbine in this study, transient effect could occur when the turbine interacts with the non-uniform wake flow. Strong fluctuation in the flow may have a significant impact on the turbine dynamic by inducing torque variation; therefore, the rotation rate of the turbine could vary according to the inertia of the total system. Additional feedback loop to account for this fluid-structure aspect of the physics would be required, demanding additional computational resources. Such physical considerations were not accounted for in the simulations.

Finally, the transient simulations where performed using a time step of 0.01 s for a total duration of 15 s (one turbine) and 20 s (two turbine).

III. SINGLE TURBINE VALIDATION/RESULTS

The metrics considered for the validation are the power and thrust coefficients, C_P and C_T respectively. They are given in Eqs. (1) and (2).

$$C_p = \frac{\omega Q}{1/2\,\rho_w A U_0^3} \tag{1}$$

$$C_T = \frac{T}{1/2\,\rho_w A U_0^2} \tag{2}$$

where Q and T are the turbine torque and thrust respectively, ρ_w is the fresh water density taken at 995 kg/m^3, ω is the rotational rate in rad/s. and A is the swept area of the turbine in m^2 given by Eq. (3). Is it important to note that both coefficients are evaluated for both turbines using the free-stream constant inlet velocity, even if the downstream turbine will see a disturbed flow having an average, and a local velocity, that will differ from the inlet value of U_0.

$$A = \pi \left(\frac{D}{2}\right)^2 \tag{3}$$

Transient simulations were performed for three tip speed ratio (TSR) values, as defined in Eq. (4):

$$TSR = \frac{\omega D}{2U_0} \tag{4}$$

The values of C_P and C_T obtained from these simulations are presented in Fig. 3 along with the results from the experimental two tank tests performed by Dorman *et al.* [11] for comparison/validation.

Figure 3 shows some discrepancies occurring between the numerical and experimental tow tank results. Even though numerical and tow tank results follow the same trend, turbine performances are slightly overestimated. The highest discrepancy was found at TSR 4.5 for C_P value, with a difference of 15%. The lowest discrepancy is for the C_T

value at TSR 4.5 with a difference of 8% compared to the measurement.

This small difference between numerically predicted and experimental values can be explained by the simplification done during the modelling process of the turbine. To that point, Currie *et al.* [9] showed that minor changes to the blade geometry (especially the trailing edge) and slight difference in boundary layer meshing on the wall of the blades, could result in significant variation of the predicted values for both C_p and C_T. Additionally, some physical phenomenon, such as hydromechanical interaction between the flow and blades, inducing load variation, vibration, potential rotational speed variation and energy loss, are neglected. Therefore, the values obtained are considered to be satisfactory regarding the approximation made on the turbine geometry and the grid selection made to reduce computational time.

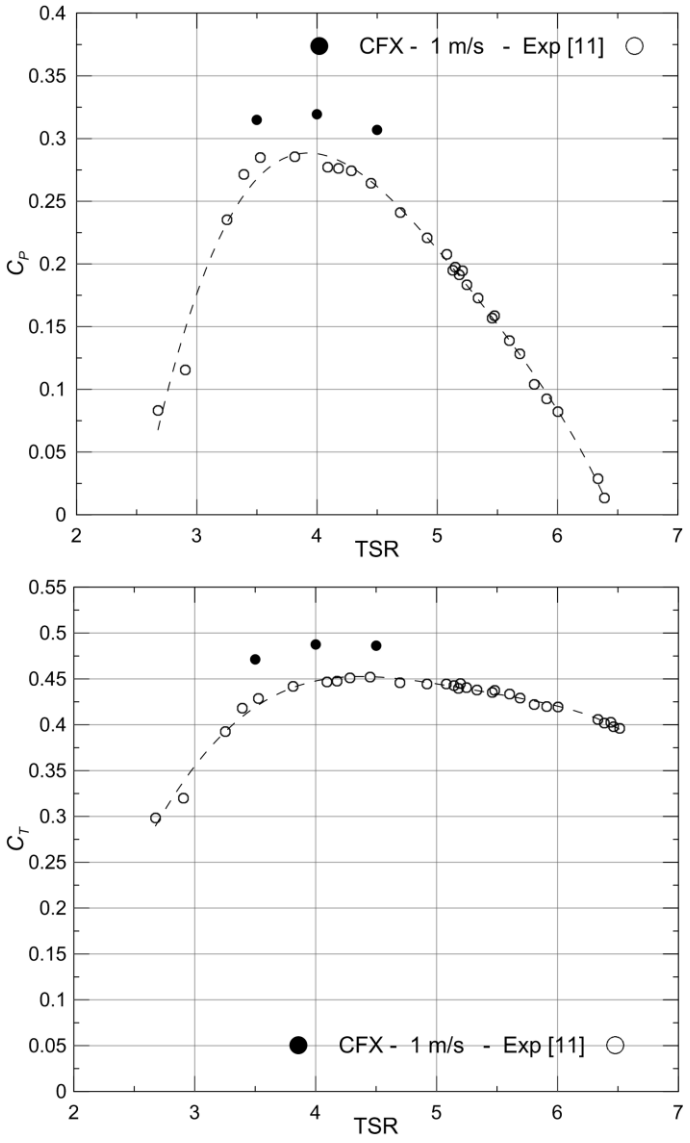

Figure 3: Numerical C_p and C_T as a function of TSR compared to experimental measurements from [11].

Once a downstream turbine is added behind this one, its performances will strongly depend on the nature of the incoming flow in the wake. Figure 4 shows the flow velocity at cross-sections situated 3*D*. 7*D* and 10*D* in the wake of the turbine; remembering that the downstream turbine will sit a distance 10*D* in the wake of this one. From Fig. 4, it is clear that the flow is far from having recovered, with a minimum velocity at 10*D* of 0.65 m/s which is 65% of the inlet velocity. It is also observed that there is a substantial region, extending more than 0.2 m in all directions around the central point of the turbine hub where the velocity remains below 0.75 m/s or at level below 75% of the inlet velocity.

Regarding the shape of the wake, a strong asymmetry can be noticed. Figure 5 points to the cause and mechanism behind this deformation of the wake. The two in-plane components *u* and *v* of the flow velocity are represented by tis vector field. A strong swirling occurs in the wake with in-plane velocity going up to 1/10th of the inlet velocity.

Specifically, when it comes to the position of the downstream turbine at 10*D*, in this study, the turbine is placed to the right of the upstream turbine when looking at the assembly from the front. From Fig. 4, this means the downstream turbine is placed on the side where the flow has recovered slightly more, but where the turbine blades will encounter a flow in the wake with velocities over a greater range, from 0.65 m/s to 1.1 m/s (the positions of the downstream turbine central hub in two of the studied configurations are shown with a green X on Fig. 4).

Outside the wake, the flow velocity sees a significant increase of 10% compared to the inlet velocity with values up to 1.1 m/s. This increase is the result of mass conservation and blockage effect, more so blockage from the turbine and nacelle, than the walls of the numerical domain.

IV. DOWNSTREAM TURBINE PERFORMANCE

Simulations looking at the interaction of the downstream turbine with the wake generated by the upstream one were performed at a TSR = 4. This value was selected since it is within the range of maximum C_p values while happening at a slower rotation rate which enables greater temporal resolution without the need for much shorter numerical time steps.

The downstream turbine power and thrust coefficients C_p and C_T have been evaluated over the last 10 turbine rotations for all three setups when the system had reach quasi-steady state (over the simulated time, the turbines had 31 complete rotations). The time evolution of both coefficients for the upstream and downstream turbine (for all three offset positions) is presented in Fig. 6 for one full rotation period.

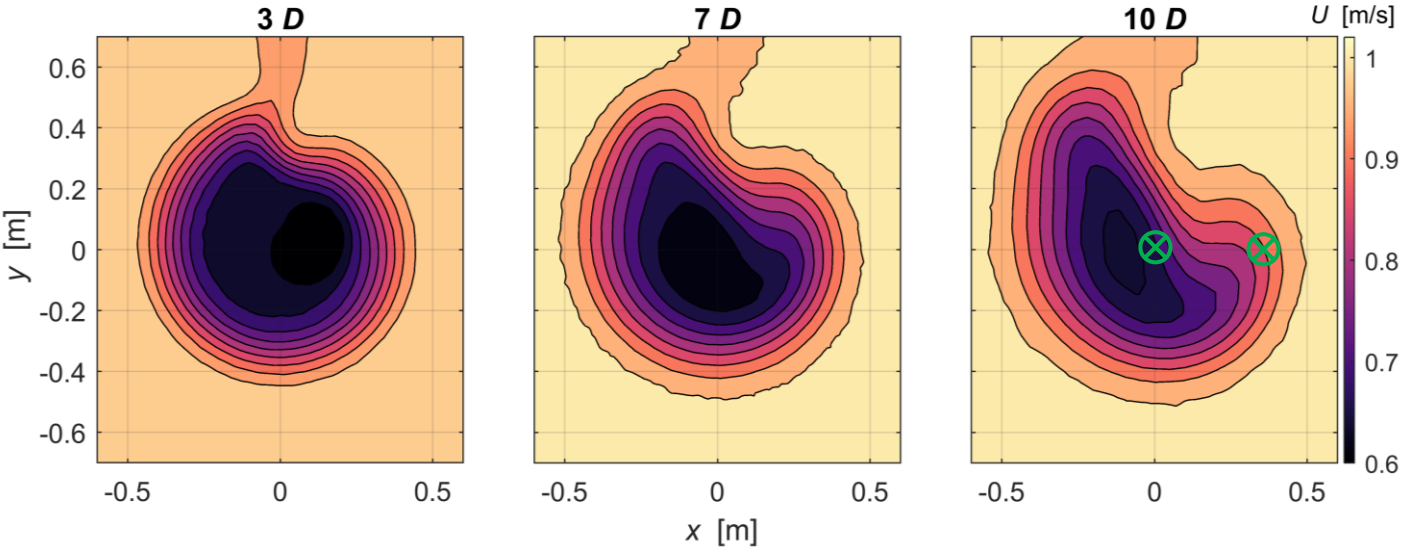

Figure 4: Wake velocity at cross-sections situated 3*D*. 7*D* and 10*D* in the wake of the turbine.

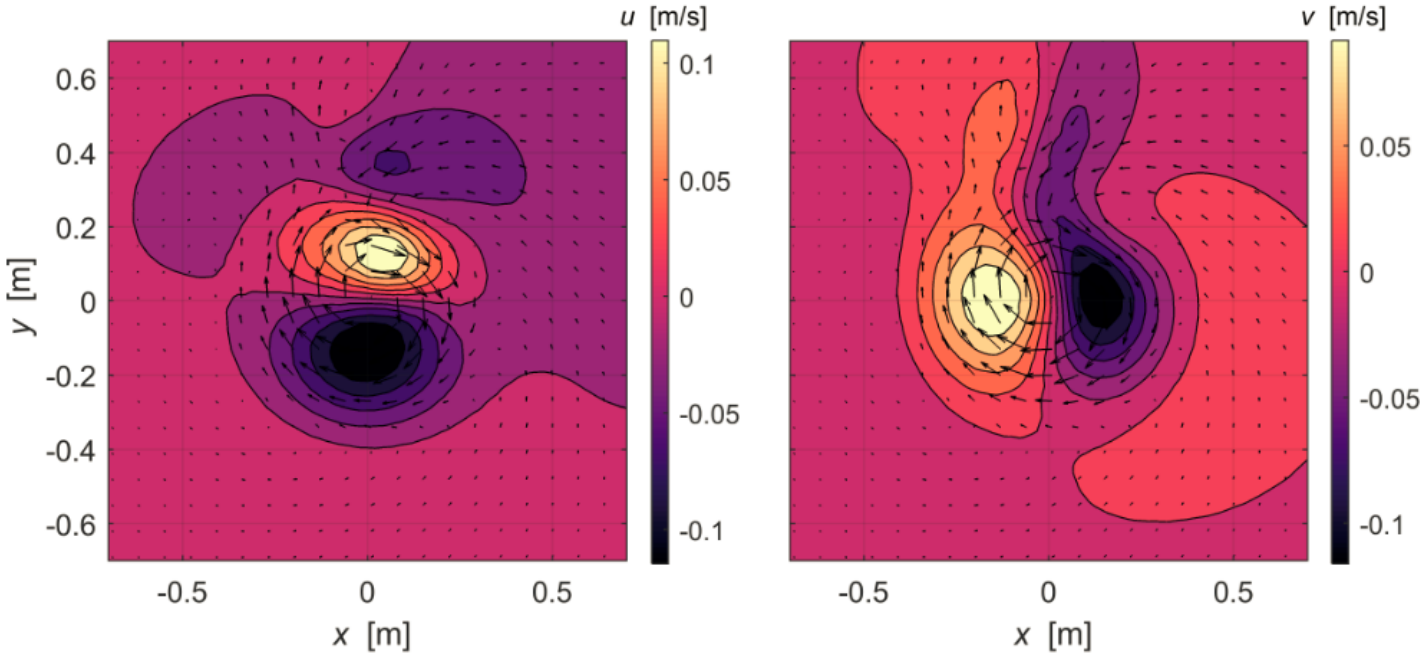

Figure 5: Velocity contour plots for *u* and *v* velocity components at 3*D* in the wake of the turbine.

The average values for each coefficient, and the absolute and relative amplitude of the fluctuation of each are presented in Table 4. First about the results, the upstream turbine performances are identical, within normal numerical uncertainty, compared to the results obtained for the single turbine simulations (0.5% difference for C_P; 0.08% for C_T). These observations are in line with what was observed by Jeffcoate *et al.* [5].

From Fig. 6 and Table 4, the 0*D* configuration leads to the lowest performance, followed by the 0.5*D* and 1*D* offsets. This is explained by the fact that with 0*D* offset, the downstream turbine essentially sees a highly turbulent flow already having a rotational component and an average velocity approximately 20 to 25% lower than the flow inlet velocity of 1 m/s (yet, the coefficients in this case are still dimensionalized using the constant inlet velocity). This clearly explains why the predicted C_p is 69% lower. This reduction goes down to 21% for the 0.5*D* offset configuration and a slight increase in C_p is observed (3%) when the downstream turbine is offset by 1*D*.

For C_T, the 0*D* configuration shows a reduction of 49% compared to the upstream turbine. The 0.5*D* configuration shows only a reduction of 15% while for 1*D*, C_T increases slightly by 2%.

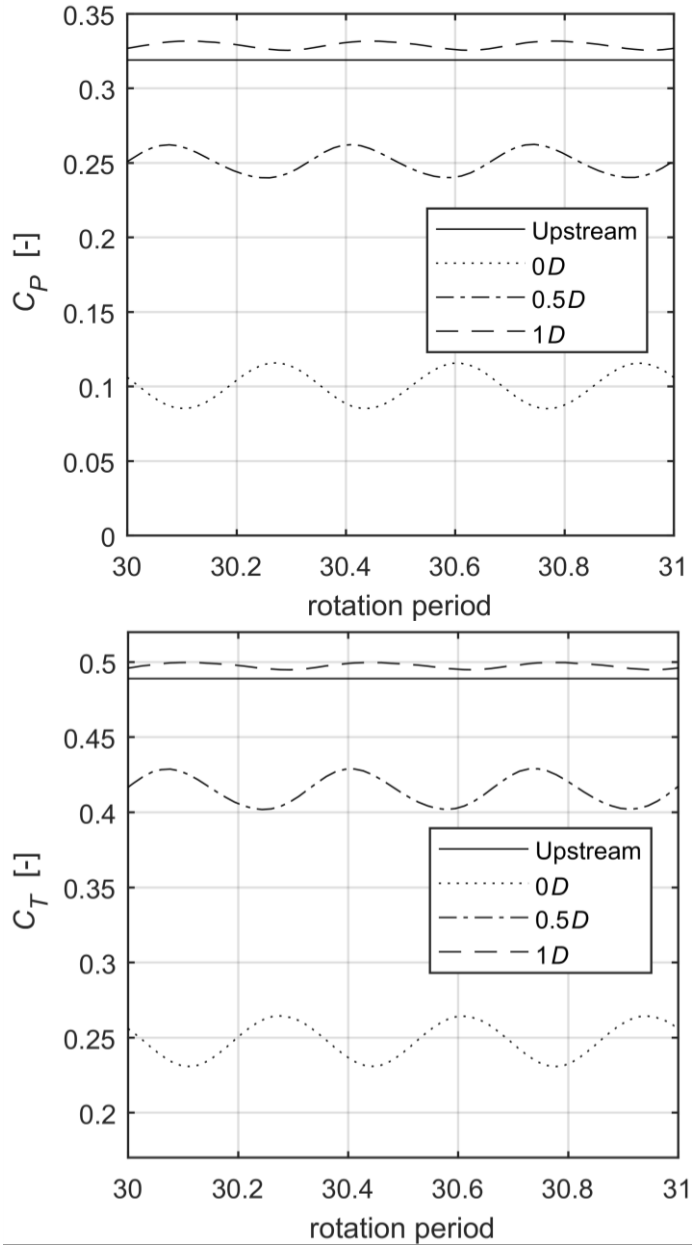

Figure 6: Numerical C_p and C_T over one rotation period at TSR = 4 for the upstream and downstream turbine for the three studied configurations.

Table 4: Upstream and Downstream Turbine Performance

	Upstream Turbine	Downstream Turbine Offset 0*D*	0.5*D*	1*D*
$\overline{C_p}$	0.3190	0.1004	0.2507	0.3288
Amplitude	-	0.0309	0.0230	0.0063
Relative Amplitude	-	30.77%	9.17%	1.91%
$\overline{C_t}$	0.4890	0.2478	0.4150	0.4975
Amplitude	-	0.0339	0.0280	0.0049
Relative Amplitude	-	13.6%	6.74%	0.98%

The increases observed in the 1*D* configuration are caused by the observed increase in wake velocity just outside of the central wake where a substantial velocity deficit is observed, as mentioned in the previous section.

Of particular interest from Fig. 6 is the oscillatory nature of both coefficients for the downstream turbine. The amplitude of the oscillation also being affected by the position of the downstream turbine in the wake of upstream one. All the time series show the same characteristics, with an oscillation period equal to 1/3rd of the rotation period of the turbine; although, the oscillation is out of phase for the three configurations. This is the result of the turbine blades experiencing the same flow but with a phase shift of ±1/3rd of the rotation period from each other. It appears that the oscillation is solely driven by the turbine rotation. The intensity of the time varying component of the incoming flow velocity in the wake is negligible compared to the local mean flow velocity and has no measurable effect on the downstream turbine performance.

The strongest amplitude of these oscillation is observed in the 0*D* configuration, with amplitudes decreasing with an increase in the offset of the downstream turbine. In the 0*D* configuration, C_p sees fluctuations of its value of over 30% above and below the average value. These variations in power extraction are happening rapidly, on a scale equal to 1/3rd of the rotation period, so less then 0.2 s for this configuration; they can potentially create issues in the energy producing and converting components of the turbine.

Even more important, from the loading/structural aspect of the blades, C_T sees fluctuations up to 13.6% around the average loading on the turbine, and its blade; again, also fluctuating over a short period. Therefore, the turbine blades will see varying local turbulent flow velocity during their rotation, which will lead to cyclical, and rapid, load variations on those blades.

The results from these simulations can be used to determine the extent of the loads, and fluctuation of those loads, on the turbine blades of the downstream turbine over time. This part of this analysis is on-going and will be presented at the Asian Wave and Tidal Energy Conference (AWTEC) later this year [14].

V. CONCLUSION

A fully transient numerical model of two three-bladed horizontal axis tidal turbines positioned one behind the other with a separation of 10*D* has been created and simulated. For a constant inlet velocity of 1 m/s, the results show that at a distance 10*D* behind the turbine, the wake still shows large areas of velocity deficit, up to 35% in velocity reduction compared to the inlet free-stream velocity. The wake also shows a large degree of asymmetry which will impact the overall performance of a second turbine downstream at this position.

When looking at the behavior of a downstream turbine, it was found that C_p and C_T were both reduced, by up to 69 and 49% respectively when the downstream turbine is offset by less than a full turbine diameter. Both power and thrust are then subjected to large and rapid fluctuations which will have an impact on energy harvesting and overall blade loading leading to fatigue.

ACKNOWLEDGMENT

The authors are thankful to the French Embassy in Canada for the France Canada Research Fund (FCRF) award that supported this work, as well as to the Canadian Foundation for Innovation (CFI) for their financial assistance regarding the computing systems and the Faculty of Engineering at Dalhousie University.

REFERENCES

[1] R. Karsten, M. O'Flaherty-Sproul, J. McMillan, J. Culina, G. Trowse, and A. Hay. "Analysis of Tidal Turbine Arrays in Digby Gut and Petit Passage, Nova Scotia," in 4th International Conference on Ocean Energy (ICOE), Dublin, 2012, 6 p.

[2] L. Hammar, S. Andersson, L. Eggertsen, J. Haglund, M. Gullstrom, J. Ehnberg, and S. Molander, "Hydrokinetic turbine effects on fish swimming behaviour," PLoS One, vol. 8, 2013, pp. e84141.

[3] T. Roc, D. Greaves, D.C. Conley, and M. Leybourne. "Optimising commercial-scale TEC arrays: genetic algorithm, Fractal & Eco-mimicry," in 10th European Wave and Tidal Energy Conference (EWTEC), Aalborg, Denmark, 2013, 12 p.

[4] G. Bai, J. Li, P. Fan, and G. Li, "Numerical investigations of the effects of different arrays on power extractions of horizontal axis tidal current turbines," Renewable Energy, vol. 53, 2013, pp. 180-186.

[5] P. Jeffcoate, T. Whittaker, C. Boake, and B. Elsaesser, "Field tests of multiple 1/10 scale tidal turbines in steady flows," Renewable Energy, vol. 87, 2016, pp. 240-252.

[6] S.R. Turnock, A.B. Phillips, J. Banks, and R. Nicholls-Lee, "Modelling tidal current turbine wakes using a coupled RANS-BEMT approach as a tool for analysing power capture of arrays of turbines," Ocean Engineering, vol. 38, 2011, pp. 1300-1307.

[7] I. Masters, R. Malki, A.J. Williams, and T.N. Croft, "The influence of flow acceleration on tidal stream turbine wake dynamics: A numerical study using a coupled BEM–CFD model," Applied Mathematical Modelling, vol. 37, 2013, pp. 7905-7918.

[8] T. Leroux, N. Osbourne, J.M. McMillan, D. Groulx, and A.E. Hay. "Numerical Modelling of a Tidal Turbine Behaviour under Realistic Unsteady Tidal Flow," in 3rd Asian Wave and Tidal Energy Conference (AWTEC), Singapore, 2016, 10 p.

[9] G. Currie, N. Osbourne, and D. Groulx. "Numerical Modelling of a Three-Bladed NREL S814 Tidal Turbine," in 3rd Asian Wave and Tidal Energy Conference (AWTEC), Singapore, 2016, 10 p.

[10] N. Osbourne, D. Groulx, and I. Penesis. "3D Modelling of a Tidal Turbine - An Investigation of Wake Phenomena," in 11th European Wave and Tidal Energy Conference (EWTEC), Nantes, France, 2015, 10 p.

[11] D.A. Doman, R.E. Murray, M.J. Pegg, K. Gracie, C.M. Johnstone, and T. Nevalainen, "Tow-tank testing of a 1/20th scale horizontal axis tidal turbine with uncertainty analysis," International Journal of Marine Energy, vol. 11, 2015, pp. 105-119.

[12] I. Afgan, J. McNaughton, S. Rolfo, D.D. Apsley, T. Stallard, and P. Stansby, "Turbulent flow and loading on a tidal stream turbine by LES and RANS," International Journal of Heat and Fluid Flow, vol. 43, 2013, pp. 96-108.

[13] J.H. Lee, S. Park, D.H. Kim, S.H. Rhee, and M.-C. Kim, "Computational methods for performance analysis of horizontal axis tidal stream turbines," Applied Energy, vol. 98, 2012, pp. 512-523.

[14] V. Podeur, D. Groulx, and C. Jochum. "Tidal Turbine Interaction: Effect of Upstream Turbine Wake on Downstream Turbine," in 4th Asian Wave and Tidal Energy Conference (AWTEC), Taipei, Taiwan, 2018, 10 p.

AUTHORS

First Author – Vincent Podeur, MSc – Research Engineer, Laboratory of Applied Multiphase Thermal Engineering (LAMTE) – Dalhousie University, vincent.podeur@gmail.com.

Second Author – Dominic Groulx, PhD - Professor, Laboratory of Applied Multiphase Thermal Engineering (LAMTE) – Dalhousie University, dominic.groulx@dal.ca.

Third Author – Christian Jochum, Associate Professor, Naval and Offshore Structures Laboratory – ENSTA Bretagne / IRDL-UMR CNRS 6027, christian.jochum@ensta-bretagne.fr.

Correspondence Author – Dominic Groulx, PhD - Professor, Laboratory of Applied Multiphase Thermal Engineering (LAMTE) – Dalhousie University, dominic.groulx@dal.ca.